European Journal of Molecular & Clinical Medicine

ISSN 2515-8260 Volume 07, Issue 11, 2020

Optical and Electronic Structure of a Double Perovskite Oxides Ca_2MnCoO_6

Ajay Kumar [1] Sujit Kumar [2] P. Poddar[3]
[1,2,3] Magadh University, Bodhgaya, India

ABSTRACT

The prime objective of the present work is evaluating the performance of double Perovskite material with Calcium in the A-site cation and Manganese and Cobalt in the B-site cation. The Ca_2MnCoO_6 the double Perovskite which is a compound of Calcium, Manganese with cobalt is made in the form of polycrystalline using the attached quartz pipe system. The partial oxygen pressure inside the quartz tube expressed this as an important set parameter for the production of a structural phase model. This parameter was controlled using the ratio between ReO_2 and ReO_3 content and the filling parameter (ratio between weight and total quartz tab content). Molecular and chemical components were investigated by scanning with electron microscopy and diffraction microscopy. The structural parameters of the crystal were determined by analyzing the X-ray powder distribution pattern with high resolution synchrotron. The analysis indicates that the sample is a single-layer compound compatible with the monolin crystal structure. (Space group $P2_1/n$) with a = 5.3649 (2) Å; b = 5.49863 (3) Å; c = 7.77524(3) Å; and β = 90.19(1)º. Computer simulations were performed considering two cation valence settings, that is, (i) $Mn^{2+}Re^{6+}$ or (ii) $Mn^{3+}Re^{5+}$, for the Ca_2MnCoO_6 compound. XANES analysis measurements indicated +2.4 for the means valence of Mn (a mixture of Mn^{2+} and Mn^{3+}) and +5.8 for the effective valence of Re (an intermediate valence between Re^{4+} (ReO_2) and Re^{6+} (ReO_3)). In summary, we concluded that Ca_2MnCoO_6 Mn and Re have a mixed valence configuration based on oxygen content of 6.0±0.2.

1. Introduction

Perovskite bodies and deformations have been tested for a long time and now again attract more attention to the colossal the magnetic resistance (CMR) properties of this type of structure. Double Perovskite is Perovskite in which all axes are doubled, increasing the volume eightfold, and the most common cause of the largest unit is the sequence of different atoms in place B in the stoichiometric of ABO_2. A in $A2B1BO_6$ and in ABO_3 compositions is often alkaline-earth (AE), and with AE (Ca) Perovskite structure distorts in a different way and adversely affects the symmetry (Valldor et al, 2006), which is often reduced to monoclinic When the center occupies a site, this excessive equilibrium is common in cubic pyruvate, but as soon as Ba is present, the tension narrows and in some cases turns hexagonal. Numerous notifications like Philip Atal. A site has studied the correlation between cation size and the characteristics of double pyruvate. The spin orbit of the Grando et al. Ion is focused on the appearance and its influence on the electronic properties of the Ca_2FeReO_6 compound.(Hereroet al., 2012). To illustrate the

magnetic and electronic results, X-ray absorption of the ferry-based double pyrovoiskets series employed in recent theoretical calculations was studied. Using X-ray magnetic circular dichotomy on the edges of the Scura etc. Reel 2.3, a considerable orbital magnetic moment was observed, which means that in a similar series of ferro-based double pyruvicites by Herrero Martin, a non- Movable orbit is a symbol of the moment. Finally, Cert et al., 2001, published a major situational review showing the importance of these substances for spontaneous devices and that the physics involved in these compounds are more complex and complete than expected. This work was proposed keeping in view the scenario in which the magnetic and electronics properties of the Ca_2MnCoO_6 double pyrosocket offer a strong correlation with the structural arrangement. The main purpose was to investigate the synthesis and crystal structure of the monophonic compound Ca_2MnCoO_6.

2. Experimental Details

Ca_2MnCoO_6 was synthesized from double Perovskite oxides CaO, MnO_2, CoO_2 and CoO_3. Calcium oxide was prepared by decomposition of CaO $CaCO_3$ (alpha acer reagent, 99.9834 ٪) which was first at 950 ° C for 24 h in a dynamic vacuum and then for 4 h under oxygen flow at 1200 C [1]. Immediately the CO fired from the furnace. Placed in a dry box. MnO2 was used as a purchase (Alpha Acer, Paratronic,. 99.9886). Both RO2 (Aldrich, 99.9%) and $RioO_3$ (Aldrich, 99.9%) powders were also used as purchases. A mixture of CaO, MnO_2, CoO_2 and CoO_3 powders in a stochametric ratio of 2: 1: 0.9: 0.1 was ground and was packed inside a dry glove box filled with organ gas. This mixture of the starting material was wrapped in gold foil and sealed in an extracted (12-2 tour) quartz tube. Due to the high pressure of RO_3 vapor at relatively low temperatures, care was taken not to overheat the sample when sealing quartz tubes in space. During the first thermal treatment, a ratio of 0.8: 0.2 between Rio 2 and Rio 3 was used to obtain partial oxygen pressure inside the quartz tube at high temperatures. The ratio between the sample mass and the internal volume of the quartz tube was defined as the filling factor ff [2]. The required filling factor was estimated to be ff0.12g / cm3 to obtain 3 times the oxygen partial pressure during the first thermal treatment at high temperatures. The partial oxygen pressure inside the quartz tube revealed that it is an important synthesis parameter for the preparation of a single structural phase sample. After the first thermal treatment at room temperature, the oxygen pressure inside the quartz tube was 850 μmHg and was measured by a home-made pressure setup with an accuracy of 25 μmHg [3]. The oxygen stomatometry of the sample was assessed by analytical equilibrium (Sartorius, model TE2145, 0.0001g accuracy), taking into account the large variations of the oxide mixture before and after thermal treatment. During the thermal treatment of quartz tube, the gas filled with organ gas was placed inside the pressure furnace at a pressure of 20 times to avoid leakage of the quartz tube [4]. The sample was sintered at 1200 ° C for a total time of 160 h with two intermediate grinding steps and finally cooled slowly in the furnace. The morphology of the particles and their chemical composition were determined using a scanning electron microscope (SEM) together with an X-ray energy dispersive spectrometer

(EDS). SEM observations were made to increase to x8,000. The electron beam energy was 20 keV, and probe current of the order of 25 μA. High resolution X-ray powder differential measurements were made at ambient pressure, using wavelength λ = 1.54044, on the D10b-XPD beam line of the Brazilian Synchrotron Light Laboratory (LNLS) in Campinas. A G (111) analyzer was placed in a goniometer attached to the Carastal 2θ arm, and a detection detector was used. Right weld purification was performed using GSAS + EXPGUI Suite [5]. The structure reported by Kato Atal was used as the initial model for payment. The peak profile function was used in conjunction with the balance correction described by Finger et al. Calculate the balance due to the beam axial bend. To calculate anisotropy at half the width of the reflections, Stephens used the two-dimensional model described by Larson and Van Dryel for crystallite size and, for anisotropic stress. The value of tolerance factor T was calculated using bond valence parameters as obtained using SPUDS simulation software. SPUDS build structures for hypothetical synthesis of compounds using computational tools where structural data is not available. Local ROO6 and MNO6 octahedral oxygen coordination was tested by ray absorption near the edge (XANES) using the DX8B-XAFS2 beam line [6]. Measurements were recorded three times at room temperature in the transmission mode at the relay II (10.540 kV) and MN edge (6.450 kV). The C (111) channel cut (2D = 6.282 Å) crystal produced a single color beam with a diameter of 600 ochm focusing at 0.005 mean (0.3 EV) resolution 7keV. The first inflection point Mn (K-edge = 6.450 keV) and Pt (LIII-edge = 11.564 keV) sheets of energy calibration XNES spectrum were used as references.

3. Results

It is clear from the analysis done on 10 different crystallites, the metal is synthesized Ca_2MnCoO_6 If the sum of the elements is considered to be 4 [4]. The results of the two different microscopes were no different from the signals. If there are no systematic errors, such as incomplete element standards, the excess of the senior cannot be easily explained. Another reason for this may be that the presence of Co causes some octahedral sites to become empty due to +4 Seriously, the result will be 2 Ca_2MnCoO_6 If Ca is +2 and Mn is +5, Co should be approximately +4.8 [8], which is higher than the expectation of an octantal coordination. If oxygen is not completely absorbed then Co +4 can certainly be, but this will contribute to the proliferation of neutrons. If Mn is only +4 and octahedral sites contain the above vacancies, the nal structure will do this Ca_2MnCoO_6.

Table 1 Atomic parameters for the joined refinement of X-ray and neutron diffraction data

Atom	x	y	z	$Beta_{iso}$ (A^2)	S.o.F.
Sr	0.27	0.27	0.27	2.36(5)	1.0
Mn1	0.4	0.4	0.4	0.3(2)	0.440(6)
Ta1	0.6	0.6	0.6	0.2(2)	0.420(6)
Mn2	0	0	0	2.1(2)	0280(6)
Ta2	0	0	0	2.1(2)	0.520(6)
O	0.2586(4)	0	0	1.98(5)	1.0

Table 2 X-ray and neutron diffraction data

R values Analysis	Fitted wRp	Rp	Bknd wRp	Rp	R^2
X-ray	0.0573	0.0465	0.0645	0.0506	0.0592
Neutron	0.00908	0.0637	0.077	0.0579	0.0973

X-ray diffraction

The pound is practically the same compound and doubling its axis (7.972 A˚) makes it possible to compare the old report with the double pyrosocket presented here. The previously reported simple pervasque has a relatively larger unit cell, which can be explained Comparing two different methods of synthesis.The compounds presented here were compounded With high pressure and high partial oxygen activity, Advanced unit causes cell compression Oxidation is indicated and thus more cation spaces. Ca_2MnCoO_6 was synthesized from double Perovskite oxides CaO, MnO_2, CoO_2 and CoO_3. Calcium oxide was prepared by decomposition of CaO $CaCO_3$ (alpha acer reagent, 99.9834 ٪) which was first at 950 ° C for 24 h in a dynamic vacuum and then for 3 h under oxygen flow at 1200 C. Immediately the CO fired from the furnace. Placed in a dry box. MnO_2 was used as a purchase (Alpha Acer, Paratronic, 99.9834 ٪). Both RO_2 (Aldrich, 99.9%) and $RioO_3$ (Aldrich, 99.9%) powders were also used as purchases. A mixture of CaO, MnO_2, ReO_2 temperature region including the magnetic transition and the FC fields are indicated.

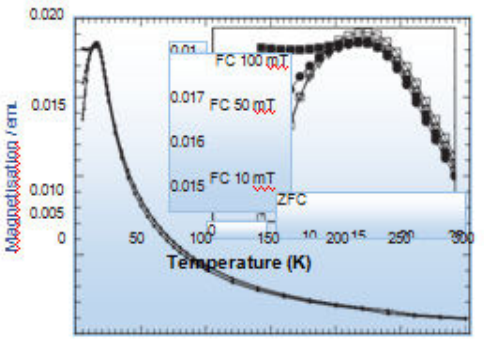

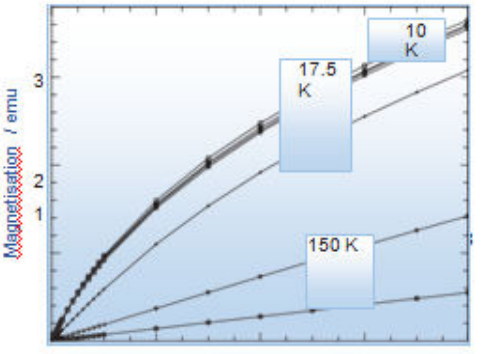

Fig. 1. The magnetization for FC and ZFC DC magnetizations. The inset displays the low

Fig. 2. Magnetization plotted as magnetization at different temperatures. The lines are added to guide the eye.

4. Discussion

The magnetic material presented here has a strong frequency dependence, as T_f changes fromK (10,000 Hz) to 17.6 K (425 Hz) correspond- ing to approximately 2.3% decrease in T_f with 25 fold change in frequency. This is supposed to put The magnetic material presented here has a strong frequency dependence, as T_f changes from 18.0 K (10,000 Hz) to 17.6 K (425 Hz) correspond- ing to approximately 2.3% decrease in T_f with 25 fold change in frequency. This is supposed to put Ca_2MnCoO_6 in between the groups of metallic and insulating spin-glasses. The resistivity (R) of Ca_2MnCoO_6 was measured with a standard four- point technique in a small temperature region below room temperature (230–280 K). R was found to increase strongly with decreasing tem- perature and had a value of 4.5 ~ 10^4 O m at 0 1C: this means that Ca_2MnCoO_6 is insulating. Interesting is also the energy loss above T_f starting from 50 K, seen as a frequency dependent change in w^{00}. Whatever happens at that point is unclear. However when comparing this fact with the magnetisation measurements at different temperatures, this event coincides with a change from paramagnetic behaviour also starting at about 50 K in the magnetisation curves. Even though the magnetic nature of this compound most likely does not give any Bragg contribution in the neutron diffraction, it would theoretically be possible to have an underlying magnetic structure which overlaps the basic structure completely. This event was tried for the low-temperature neutron (LTN) data, i.e. an anti-ferromagnetic structure was refined with the same periodicity as the double Perovskite. This demands, of course, that the symmetry of the magnetic structure correlates with the basic structure. However, the LTN data refinement including a magnetic part did not result inanything

reasonable. Taking all different observations into considera- tion it is safe to assume that the Mn has a mixed oxidation state between +3 and +4. In an octahedra the Mn^{3+} (d^4) has one electron in the orbitals pointing towards the oxygen ligands, while Mn^{4+} (d^3) lacks this electron and has only what is common for both ions: half-filled orbitals between the ligands. These two ions will naturally be involved to different extents in the super- exchange and double-exchange mechanisms. If only one of the oxidation states is responsible for the properties, the percolation limit has to be taken into question.

The material exhibits a whole range of magnetic states and starting from the paramagnetic range it has a strong ferromagnetic character, which continues down to some point between 100 and 50 K, where the maximum w is seen. The high- temperature ''ferromagnetic'' part is probably a result of one magnetic substructure, which, due to percolation is too weak and does not couple long- ranged in the measured temperature range, i.e. the concentration of the involved ions is too low and only temporary ferromagnetic interactions can be found distributed in the material. At lower temperatures, another effect starts to grow and it is likely that the anti-ferromagnetic super-ex- change mechanism compete with the double- exchange down to T_f, where large part of the magnetic structure freezes over a broad tempera- ture range, giving frequency dependency in T_f. This is an alternative explaination to the site- disordered materials, where geometrical frustra- tion is reached for the spins, due to the disadvan- tageous distribution of different oxidation states. The Ca_2MnCoO_6 can therefore be described as containing two competing magnetic mechanisms causing frustration and a gradual ''freezing'' of the spins. Ca_2MnCoO_6 in between the groups of metallic and insulating spin-glasses. The resistivity (R) of Ca_2MnCoO_6 was measured with a standard four- point technique in a small temperature region below room temperature (230–280 K). R was found to increase strongly with decreasing tem- perature and had a value of 4.5 ~ 10^4 O m at 0 1C: this means that Sr_2TaMnO_6 is insulating.

Interesting is also the energy loss above T_f starting from 50 K, seen as a frequency dependent change in w^{00}. Whatever happens at that point is unclear. However when comparing this fact with the magnetisation measurements at different temperatures (Fig. 6), this event coincides with a change from paramagnetic behaviour also starting at about 50 K in the magnetisation curves. Even though the magnetic nature of this compound most likely does not give any Bragg contribution in the neutron diffraction, it would theoretically be possible to have an underlying magnetic structure which overlaps the basic structure completely. This event was tried for the low-temperature neutron (LTN) data, i.e. an anti-ferromagnetic structure was refined with the same periodicity as the double Perovskite. This demands, of course, that the symmetry of the magnetic structure correlates with the basic structure. However, the LTN data refinement including a

magnetic part did not result in anything reasonable.

Taking all different observations into considera- tion it is safe to assume that the Mn has a mixed oxidation state between +3 and +4. In an octahedra the Mn^{3+} (d^4) has one electron in the orbitals pointing towards the oxygen ligands, while Mn^{4+} (d^3) lacks this electron and has only what is common for both ions: half-filled orbitals between the ligands. These two ions will naturally be involved to different extents in the super- exchange and double-exchange mechanisms.

If only one of the oxidation states is responsible for the properties, the percolation limit has to be taken into question. The material exhibits a whole range of magnetic states and starting from the paramagnetic range it has a strong ferromagnetic character, which continues down to some point between 100 and 50 K, where the maximum w is seen. The high- temperature ''ferromagnetic'' part is probably a result of one magnetic substructure, which, due to percolation is too weak and does not couple long- ranged in the measured temperature range, i.e. the concentration of the involved ions is too low and only temporary ferromagnetic interactions can be found distributed in the material. At lower temperatures, another effect starts to grow and it is likely that the anti-ferromagnetic super-ex- change mechanism compete with the double- exchange down to T_f, where large part of the magnetic structure freezes over a broad tempera- ture range, giving frequency dependency in T_f. This is an alternative explaination to the site- disordered materials, where geometrical frustra- tion is reached for the spins, due to the disadvan- tageous distribution of different oxidation states. The Ca2MnCoO6 can therefore be described as containing two competing magnetic mechanisms causing frustration.

References

[1] E.G. Fesenko, V.S. Filip'ev, M.F. Kupriyanov, Izvestiya akademii nauk SSSR, Seriya Fizicheskaya 28 (1964) 669.

[2] M.F. Kupriyanov, V.S. Filip'ev, Kristallografiya 8 (1963) 356.

[3] B. Raveau, A. Maignan, C. Martin, M. Hervieu, Chem. Mater. 10 (1998) 2641.

[4] O. Bock, U. Mu¨ller, Acta Cryst. B 58 (2002) 594.

[5] P.D. Battle, T.C. Gibb, A.J. Herod, S-H. Kim, J. Mater. Chem. 5 (6) (1995) 685.

[6] A. Morawski, A. Paszewin, T. Lada, H. Marciniak, K. Przybylski, H. Szymczak, A. Wisniewski, Trans. Appl. Superc. 7 (2) (1997) 1903.

[7] K.E. Johansson, T. Palm, P-E. Werner, J. Phys. E: Sci. Instrum. 13 (1980) 1289.

[8] P-E. Werner, Ark. Kemi. 31 (1969) 513.

[9] A.C. Larson, R.B. Von Dreele, LANSCE, MS-H805, Los Alamos National Laboratory, Los Alamos, NM 87545.

[10] C. Keller, Inorg. Chem. 1 (1962) 790.

[11] M.F. Kupriyanov, E.G. Fesenko, Kristallografiya 7 (1962) 315.

[12] J-H. Choy, J-H. Park, S-T. Hong, D-K. Kim, J. Solid State Chem. 111 (1994) 370.

[13] S. Tao, J.T.S. Irvine, J. Mater. Chem. 12 (2002) 2356.

[14] J.N. Reimers, J.E. Greedan, C.V. Stager, M. Bjorgvinnsen, M.A. Subramanian, Phys. Rev. B 43 (7) (1991) 5692. [15] C. Zener, Phys. Rev. 82 (1951) 403.

[9] C.A.M. Mulder, A.J. van Duyneveldt, J.A. Mydosh, Phys. Rev. B 23 (3) (1981) 1384.

[10] C.A. Cardoso, F.M. Araujo-Moreira, V.P.S. Awana, E. Takayama-Muromachi, O.F. de Lima, H. Yamauchi, M. Karppinen, Phys. Rev. B 67 (2003) 020407-1.

[11] A. Chakravarti, R. Ranganathan, S.B. Roy, Phys. Rev. 46 (10) (1992) 6236.

[12] H.B.G. Casimir, F.K. du Pre´, Physica 5 (1938) 507. [20] [a] H. Vogel, Phys. Z 22 (1921) 645;

European Journal of Molecular & Clinical Medicine

ISSN 2515-8260 Volume 07, Issue 11, 2020

ISSN 2515-8260 Volume 07, Issue 11, 2020